# EQUILIBRIUM JOURNAL OF CHEMICAL ENGINEERING

Homepage: https://jurnal.uns.ac.id/equilibrium



1

# Synthesis and Characterization of Novel Bi-Functional Catalyst from Mixture of Agro-Wastes Using Hydrothermal-Sulphonation Method

Ifeanyi Michael Nwachukwu<sup>a</sup>, Wisdom Chukwuemeke Ulakpa<sup>b\*</sup>, Odeworitse Eyide<sup>c</sup>, Josephine Eguare Ekpenkhio<sup>d</sup>, Christopher Ehiaguina Akhabue<sup>a</sup>

<sup>a</sup>Department of Chemical Engineering, University of Benin, Benin City, 300283, Nigeria
<sup>b</sup>Department of Chemical Engineering, Southern Delta University of Science and Technology, Ozoro, 334113, Nigeria
<sup>c</sup>Department of Chemical Engineering, University of Delta, Agbor, 321103, Nigeria
<sup>d</sup>Department of Industrial and Systems Engineering, University of Alabama, Huntsville(UAH), 35899, United States

\*Corresponding author: ulakpa.wisdom@yahoo.com, ulakpawc@dsust.edu.ng

DOI: https://dx.doi.org/10.20961/equilibrium.v9i2.101280

Article History

Received: 22-04-2025, Accepted: 14-11-2025, Published: 22-11-2025

#### **Keywords:**

Bi-functional, Cocoa pods, Eggshells, Snailshells, Orange peels ABSTRACT. This research illustrates the development of a bi-functional catalyst derived from a blend of agricultural waste materials, employing a hydrothermal method. The precursor materials included cocoa pods, eggshells, snail shells, and orange peels. The resulting bi-functional catalyst underwent characterization through a variety of techniques, such as FTIR, XRF, XRD, SEM, TGA-DTA, and both single-point and multi-point BET analyses. The FTIR and XRD analyses distinctly indicated the transformation of calcium carbonate (CaCO<sub>3</sub>) from the agro-waste precursors into calcium oxide (CaO). XRD further validated the crystalline structures and identified the oxide minerals present within the catalyst using an X-ray diffractometer. The DTA-DSC curve displayed notable endothermic peaks at 400 °C, indicating a decomposition reaction that leads to the formation of a new compound. The surface area of the bi-functional catalyst was assessed using single-point and multi-point Brunauer-Emmett-Teller (BET) methods, yielding values of 87.94 m<sup>2</sup>/g and 159.4 m<sup>2</sup>/g, respectively. Additionally, the adsorption surface area of the catalyst's pore size was measured at 165 m<sup>2</sup>/g, while the Langmuir surface area was found to be 2792 m<sup>2</sup>/g, as determined by the Barrett-Joyner-Halenda (BJH) method. The mean pore volume was calculated to be 812.5 cc/g, and the average pore diameter was 2.138 nm, as established through BJH analysis. The diverse surface property results underscore the substantial influence of surface area on the catalyst's activity, as a larger surface area facilitates more efficient interactions between reactants and active sites. Consequently, the agricultural waste materials represent a promising source of calcium oxide for various applications across numerous scientific and engineering disciplines.

#### 1. INTRODUCTION

The pursuit of sustainable and eco-friendly catalytic solutions has sparked interest in utilizing agricultural waste as potential raw materials for catalyst production [1]. Given their abundance, renewability, and frequent underutilization, agro-wastes offer a remarkable opportunity to create high-value products with minimal environmental repercussions [2-3]. In Nigeria alone, around 12 million tonnes of agricultural waste shells are improperly disposed of each year, leading to significant environmental and health challenges [4]. These wastes encompass periwinkle shells, cockle shells, snail shells, oyster shells, and eggshells [5-6]. Recent studies have indicated that biomaterials from eggshells and snail shells can serve as effective precursors for the synthesis of heterogeneous catalysts.

Moreover, agro-waste biomass such as cocoa pods and orange peels, often generated as by-products during agricultural activities, can also be utilized as precursor materials for catalyst preparation [7]. The potential of agrowastes to serve as precursors for heterogeneous catalysts is largely attributed to their high calcium content, which contributes to significant catalytic activity. This approach not only offers a cost-effective solution but also provides environmental advantages and effective yields in fatty acid methyl ester production [8].

Heterogeneous catalysts are essential in a range of industrial processes, including chemical synthesis, environmental cleanup, and energy generation [9]. The advancement of solid heterogeneous catalysts that exhibit bifunctional characteristics—possessing both acidic and basic sites can greatly improve efficiency, selectivity, and longevity for various industrial applications [10-11]. Recently, there has been a surge of interest within the scientific community regarding solid heterogeneous catalysts due to the demand for high-performance catalysts

produced through synthesis methods that ensure uniform pore size distribution, extensive specific surface area, high alkalinity, and optimal dispersion of active metals on precursor materials [10-12]. These attributes are crucial as they enhance the available surface area for reactions and guarantee consistent catalytic performance. To achieve these goals, researchers have explored a range of cost-effective and innovative preparation methods that extend beyond traditional techniques [12].

The method used to prepare catalysts is crucial, as it greatly affects both their physicochemical characteristics and overall effectiveness [12]. Conventional methods for catalyst production typically depend on finite resources and are often energy-intensive. In contrast, the hydrothermal approach presents an environmentally friendly alternative by using water under subcritical or supercritical conditions to transform raw materials into functional catalysts. This technique boasts several advantages over other methods for producing bi-functional catalysts, such as the ability to precisely control essential factors like particle size, morphology, crystallinity, simplicity, cost efficiency, and operation at lower temperatures and pressures [13]. It is important to emphasize that characterizing the synthesized catalyst is vital for understanding its structure, surface characteristics, and catalytic performance. Various analytical techniques, including X-ray diffraction (XRD), X-ray fluorescence (XRF), scanning electron microscopy (SEM), Fourier transform infrared spectroscopy (FTIR), thermogravimetric analysis (TGA)/differential thermal analysis (DTA), and Brunauer-Emmett-Teller (BET) surface area analysis, will be utilized to assess the material's properties and evaluate its potential for industrial applications [14-15].

Conclusively, this research seeks to create an innovative bi-functional catalyst by utilizing a combination of agricultural waste through hydrothermal methods and sulphonation reactions. By converting agricultural by-products into useful catalytic materials, this study tackles the issue of waste valorization while also fostering the development of sustainable and efficient catalysts for diverse industrial uses. The effective synthesis and characterization of this catalyst could greatly enhance the domains of green chemistry and sustainable catalysis, encouraging environmentally conscious and economical solutions.

# 2. MATERIALS AND METHODS

### 2.1. Materials

Cocoa pods and Snail shell were locally sourced from a farm in Edo state, Nigeria. While the Orange Peels were sourced locally from Uselu Market, Benin City, Edo State, Nigeria and the Eggshells were sourced locally from Efosxy Baking /Catering Services, Uselu, Benin City, Edo State, Nigeria. For the research, deionized water (H2O) was used with a significant purity level of 99%. Also, all the chemicals used in the experiments were of analytical standard.

### 2.2. Methods

Snail shells, eggshells, cocoa pods, and orange peels were cleaned and properly sun-dried for 2 days at an average temperature of about 30 °C to reduce the moisture content. They were subsequently oven-dried at 60°C for 24 hours, after which each of the individual precursor materials was pulverized using a grinding machine separately. Equal masses of the eggshell and snail shell, which served as the alkaline precursors, were pre-treated with a 1M solution of Sodium Hydroxide (NaOH) for 48 hours. After this, they were oven-dried at 50°C for 24 hours. It was then calcined in the muffle furnace at 900°C for 6 hours. Also, an Equal mass of the Cocoa pods and the orange peels, which served as the acid precursor, were pre-treated with phosphoric acid for 48 hours, then oven-dried at 50°C. It were then carbonized at 450°C for a period of 3 hours. Furthermore, both materials were kept in a desiccator and stored in separate airtight containers. Catalyst synthesis was done using blending ratios of 1:1, 1:2, 2:1, and 3:2 for acid and alkaline precursors via wet impregnation method with functionality enhancement by suphonation process with H<sub>2</sub>SO<sub>4</sub>. The precursors were sulphonated at a temperature of 150°C to infuse the SO<sub>3</sub><sup>2-</sup> ions on the active sites of the acid precursor with corresponding mixing using a hot plate magnetic stirrer for 3h. The resulting catalyst was oven-dried at a temperature of 85°C until it is fully dried. The impregnated catalyst was ground into a powder using a grinding machine, thereafter sieved through a 500-micron sieve, and kept in an airtight desiccator. Finally, the samples were characterized.

2.3 Possible reactions accelerated by the proposed Bi-functional catalyst: cocoa pods, eggshells, snail shells, and orange peels

Bifunctional catalysts derived from cocoa pods, eggshells, snail shells, and orange peels possess both acidic and basic active sites (including Lewis acid/base sites), allowing them to accelerate a diverse range of catalytic

reactions. These reactions may include: Esterification reactions, Transesterification reactions, Condensation reactions, Hydrolysis reactions. Table 1 summarizes the potential reactions enhanced by these bifunctional catalysts derived from cocoa pods, eggshells, snail shells, and orange peels.

**Table 1**. Possible reactions accelerated by: cocoa pods, eggshells, snail shells, and orange peels bi-functional catalyst

Biomass Source	Active Sites	Accelerated Reactions		
Cocoa Pods	Acidic-basic groups (-COOH, -OH)	Esterification, transesterification, hydrolysis		
Eggshells	Basic CaO (O <sup>2-</sup> , Ca <sup>2+</sup> )	Transesterification, saponification, catalytic cracking		
Snail Shells	Basic CaO	Transesterification, saponification, catalytic cracking		
Orange Peels	Acidic-basic carbon materials	Esterification, hydrolysis, dehydration		

# 2.4. Characterization of the synthesized bi-functional catalyst

Various scientific methodologies were employed for this study. The techniques employed in this study were Fourier transform infrared spectroscopy (FTIR), X-ray fluorescence (XRF), X-ray powder diffraction (XRD), scanning electron microscopy (SEM), thermogravimetric analysis (TGA), differential thermal analysis (DTA), Barrett-Joyner-Halenda (BJH) model, and Brunauer-Emmett-Teller (BET) method. X-ray diffraction (XRD) was employed to perform crystallographic analysis of the catalyst, as well as to identify the oxide minerals present. This was achieved by producing x-rays in an x-ray tube and showing them on a screen using an x-ray diffractometer fitted with a copper anode, within an angular range of 100 < 20 < 700. In order to examine the surface structure of the catalyst that was produced, a technique known as scanning electron microscopy (SEM) investigation was employed. It also determined the dimensions and form of the particles that were supported. The SEM examination was conducted using an electron microscope operating in the 15kV - Image mode, together with a full backscatter electron (BSD) detector. The examination was performed at a field of view (FOV) of 537 m.

Fourier transform infrared (FTIR) spectroscopy was employed to analyze the functional groups, structure, and bonds present on the catalyst's surface using infrared light with wavelengths ranging from 600 to 4000cm $^{-1}$ . The X-ray fluorescence analysis was employed to ascertain the elemental composition of the catalyst produced. This was achieved by measuring the fluorescent x-ray emitted from the catalyst sample when it was stimulated by an x-ray source, using an x-ray spectrophotometer. Tungsten carbide was used to grind and mill to avoid contamination and ensure particle size is < 50  $\mu$ m to minimize heterogeneity effects in XRF analysis. For MN4, additional grinding may be needed due to potential hardness differences which may be due to high  $K_2O$ ,  $Al_2O_3$ , and MgO. Additionally, the Brunauer-Emmett-Teller (BET) analysis was utilized to investigate the specific surface area and distribution of porosity in the solid matter. The BET surface area can be measured within a range of 0.10 to 2,000 m²/g. Ultimately, thermal analysis was conducted utilizing TGA analysis. The weight loss and temperature are monitored over time as the components of the catalyst evaporate.

#### 3. RESULTS AND DISCUSSION

# 3.1. Fourier transform infrared (FTIR) analysis

Figure 1 illustrates the FTIR analysis conducted on the bi-functional catalyst. The spectra showed several absorption bands at specific wavenumbers: 3485.1 cm<sup>-1</sup>, 1801.2 cm<sup>-1</sup>, 1781.0 cm<sup>-1</sup>, 1511.8 cm<sup>-1</sup>, 1470.5 cm<sup>-1</sup>, 1103.3 cm<sup>-1</sup>, 878.9 cm<sup>-1</sup>, and 725.4 cm<sup>-1</sup> as depicted in Table 2. The sharp absorption band observed at 3485.1 cm<sup>-1</sup> can be attributed to the stretching vibrations of hydroxyl (O-H) groups. The main groups in the catalyst are the O-H and S=O groups. The O-H group results from calcium hydroxide, which is produced when atmospheric moisture reacts with calcium oxide obtained from calcinated snail shells, and the S=O group is derived from the sulphate ion infused into the acid precursor during the sulphonation process.

**Table 2.** Major absorption peaks with their functional groups and bond types.

Wave number (cm <sup>-1</sup> )	Nature of frequency	Nature of bond	Functional group
3485.1	Strong and sharp	O-H (free)	Alcohols, phenols
1470.5	Medium	C-C (in-rings)	aromatics
878.9	Strong	C-H bending	Alkene

1103.3	Strong	C-O stretching	Alcohol
1875.4	Strong	S=O stretching	Sulfone
1470.5	Medium	C-H bending	Alkane
1781.0	Strong	C=O	cyclopentanone
1511.8	Medium	C=C	Cyclic alkene

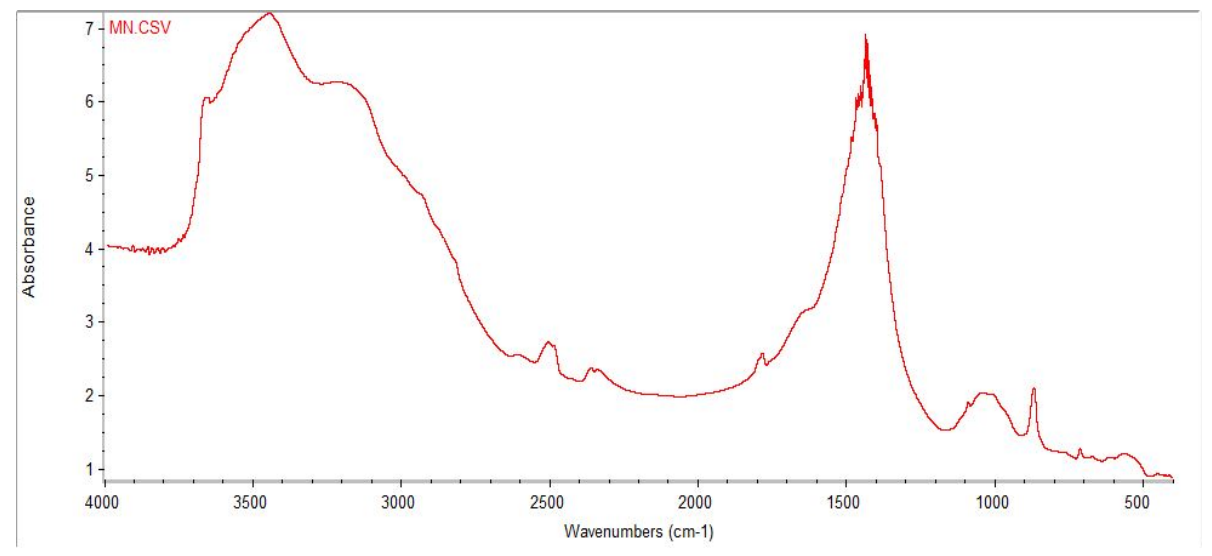


Figure 1. FTIR of bi-functional catalyst

# 3.2. X-ray fluorescence (XRF) analysis

Table 3 depicts the elemental composition oxides obtained from XRF analysis. The results obtained from the assessment of the bi-functional catalyst indicated the presence of acidic oxides (SO<sub>3</sub> and P<sub>2</sub>O<sub>5</sub>), basics oxides (CaO, MgO, Na<sub>2</sub>O and K<sub>2</sub>O) and amphoteric (Al<sub>2</sub>O<sub>3</sub> and Fe<sub>2</sub>O<sub>3</sub>) oxides. The major components present in the XRF analysis of the catalyst were SO<sub>3</sub> (15.345%), CaO (13.253%) and K<sub>2</sub>O (2.352%). To ensure that the X-ray Fluorescence (XRF) analysis accurately represents the entire population of the given samples (MN1, MN2, MN3, MN4), proper sample preparation and homogenization are critical. The compositional variations observed in the table (e.g., high SO<sub>3</sub> in MN1-MN3 vs. low in MN4, varying alkali oxides, and trace elements) suggest that the materials may be heterogeneous. To justify that the sample represents the entire population, MN1-MN3 (High SO<sub>3</sub>, CaO, P<sub>2</sub>O<sub>5</sub>) likely represent gypsum-rich or phosphogypsum materials to ensure complete homogenization to avoid sulfate segregation.MN4 (High K<sub>2</sub>O, Al<sub>2</sub>O<sub>3</sub>, Cl) suggests a clay or potash-rich component. Trace Elements; Bi, Pb, As, Sn, contamination during grinding is checked using high-purity mills.

Table 3. Percentage oxides in the Bi-functional catalyst.

Elements	Composition	Composition	Composition	Composition
	(%) MN1	(%) MN2	(%) MN3	(%) MN4
Fe <sub>2</sub> O <sub>3</sub>	0.02710	0.01664	0.06611	0.09033
CuO	0.000764	0.000991	0.001183	0.004182
NiO	0	0.02293	0.00204	0.01711
ZnO	0.000229	0.000390	0.000620	0.002611
$Al_2O_3$	0.01908	0	0.03166	0.20512
MgO	0.2013	0.0988	0.2896	0.7609
$Na_2O$	0.160	0.163	0.108	0
$SO_3$	20.735	18.536	21.836	0.27238
$P_2O_5$	0.1760	0.1105	0.2564	0.52934
CaO	14.314	13.6065	15.277	9.8156
K <sub>2</sub> O	0.2065	0.12270	0.4259	8.6540

MnO	0.00271	0.000070	0.005901	0.014689
Rb <sub>2</sub> O	0.000498	0.000387	0.000997	0.00972
SrO	0.05466	0.04968	0.05845	0.04675
Br	0.00015	0	0.00024	0.00102
Cl	0	0	0	0.1092
$Cr_2O_3$	0.00489	0.00225	0.00687	0.03069
$V_2O_5$	0	0	0	0.000285
$MoO_3$	0	0	0	0.000223
$WO_3$	0.00007	0.00704	0.00241	0.0210
$\mathrm{Bi}_2\mathrm{O}_3$	0.007	0.039	0.021	0.073
BaO	0.2126	0.0827	0.4040	0.0938
PbO	-0.001	-0.020	0.004	-0.030
$SnO_2$	0.50	0	0	0.20
$SiO_2$	0	0	0.34	0
$As_2O_3$	0	0	0.0003	-0
$Nb_2O_5$	0093	0.0399	0.0149	0.0312
$Ta_2O_5$	0	0.00065	0	0.00141
Ga	0	0.0021	1	0.0230
Ti	0.3100	0.2194	105	0.3080

# 3.3. X-ray diffraction (XRD) analysis

Using the XRD analysis, the oxides located in the catalyst along with their peak response values and crystalline nature were analyzed as shown in Figure 2. The XRD chromatograph of the catalyst in counts and 20 positions as well as the peak patterns of the various resident oxides are showed in Figure 2. With peaks at 33.449°, 43.516°, 44.498°, 46.611°, 47.813°, 50.061°, 52.425°, 53.160°, 58.504°, 60.067°, 61.179°, 65.038°, 66.281°, and 68.840°, respectively. They represents the presence of dipyramidal orthorhombic Brownmillerite, Ca(Al, Fe)<sub>2</sub>O<sub>5</sub>, as seen in Figure 2. The presence of trigonal calcite, CaCO3 is indicated by peaks at 23.166°, 31.622°, 40.395°, 43.516°, 47.813°, 48.767°, 58.504°, 61.179°, and 65.038°, respectively. Peaks at 26.696°, 40.395°, 50.061°, 60.067°, and 68.840 ° indicate the presence of tetrahedral Quartz, SiO4 implying the catalyst has a somewhat crystalline structure. While peaks 31.418°, 45.028°, 53.160°, and 66.281° indicate the presence of hexoctahedral (cubic) Oldhamite, (Ca, Mg)S.

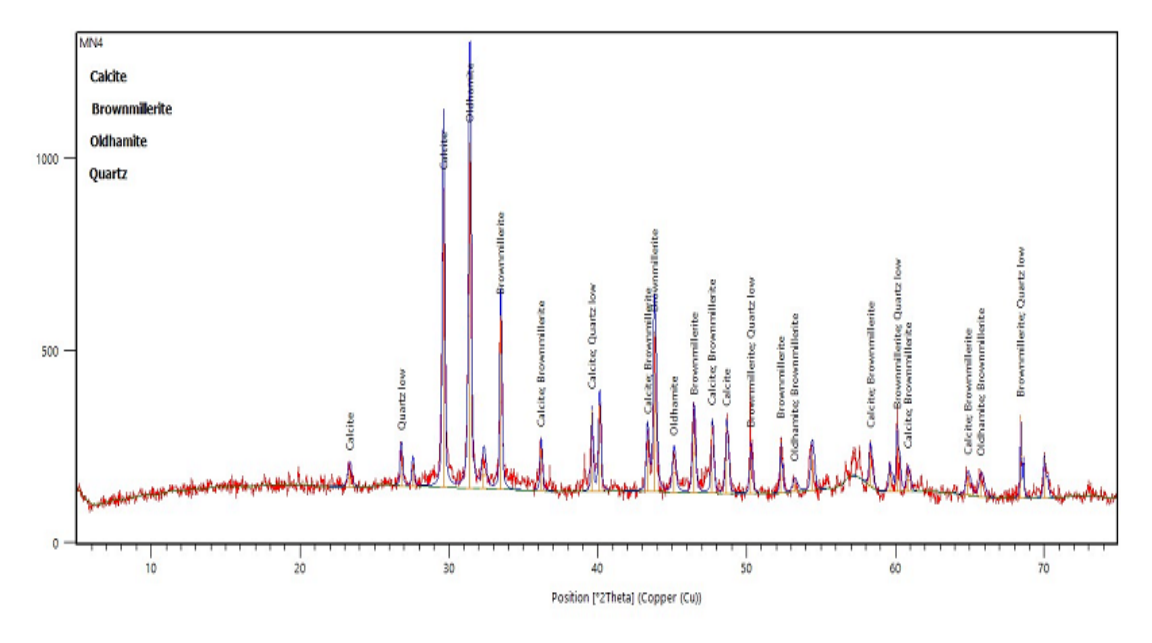


Figure 2. XRD pattern of synthesized bi-functional catalyst

# 3.4. Scanning electron microscopy (SEM) analysis

Figure 3 revealed the SEM analysis of the various catalysts employed in this process. The images were taken at different electronic lens magnifications of 200, 100, 80 and 50  $\mu$ , respectively. The analysis of the catalyst in Figure 3 (a) and Figure 3(b) showed the pore size distribution to be non-uniform and irregular, while there appeared to be an agglomeration of certain tiny-sized particles. The irregular surface of the catalyst and the finer particle agglomeration at the fringes indicate a large surface area for reactions to take place as well as numerous active catalytic sites, which will enhance and promote biodiesel yield. The SEM images in Figure 3(c) and Figure 3(d) show deep ravines, which are synonymous with pore spaces with significant sizes. According to [14], the porosity is attributed to the release of a significant amount of gaseous water molecules. This large pore is due to the sulfonation process and is believed to contribute to the catalytic activity [16].

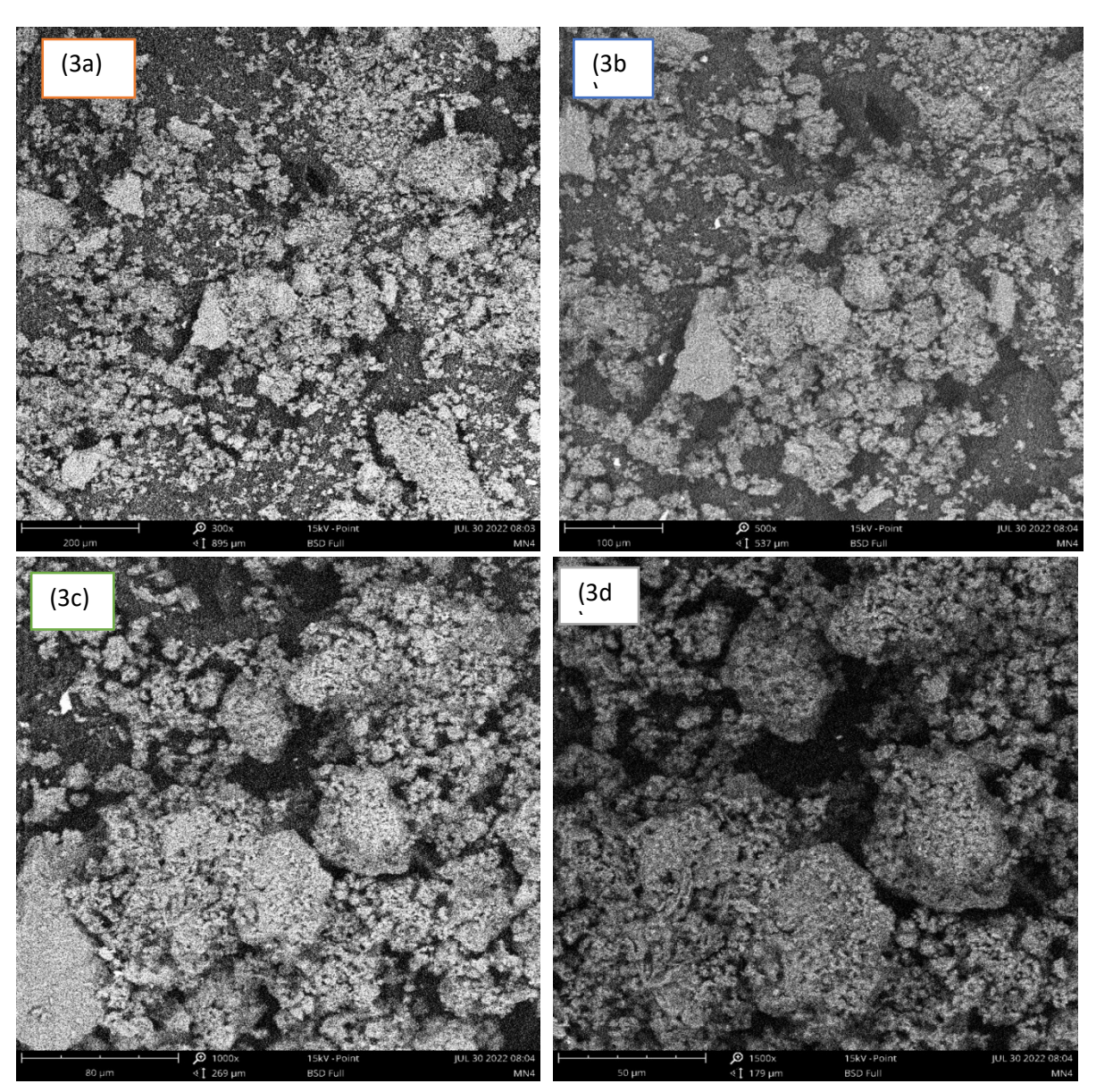


Figure 3. SEM image of bi-functional catalyst

# 3.5 Thermogravimetric analysis (TGA)/ differential thermal analysis (DTA)

The line graph in Figure 4 shows the result of the Thermo gravimetric analysis (TGA) and Differential Thermal Analysis (DTA) of the bi-functional catalyst sample. It was clear from the plot that as the temperature increases, there is a corresponding overall rate of weight loss. However, there was a sharp increase in the reduction of catalyst loading between the temperature range of 294.89°C and 485.3°C which amounted 67% of the overall catalyst weight was lost. Also, the weight loss decreases as a result of increase in temperature remains fairly constant and

steady. The weight loss can be attributed to the breakdown of carbonic precursor, resulting in the formation of carbon monoxide (CO) and carbon dioxide (CO<sub>2</sub>), as well as the removal of water from calcium hydroxide (Ca(OH)<sub>2</sub>) and the disintegration of calcium carbonate (CaCO<sub>3</sub>) [17].

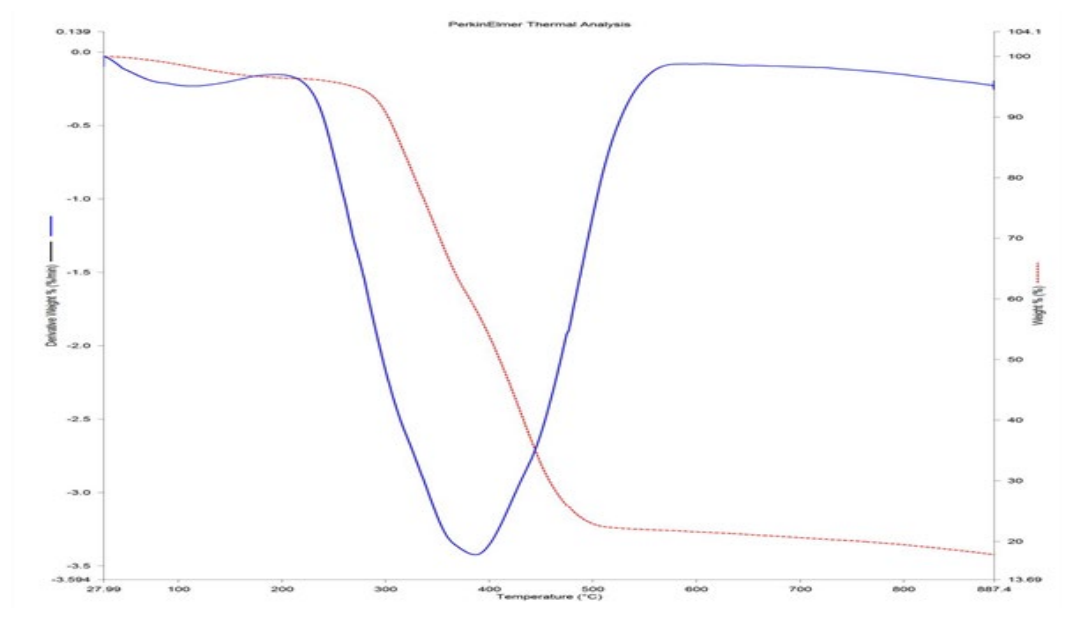


Figure 4. TGA/DTA plot for the Bi-functional Catalyst: Heat from 30°C to 950°C at 10°C/min .

# 3.6. Surface properties of the bi-functional catalyst

# 3.6.1. Surface Area

The Single Point and Multi Point Brunauer–Emmett–Teller (BET) surface area of the catalyst is shown in Figure 5 and was calculated to be  $87.94~\text{m}^2/\text{g}$  and  $159.4~\text{m}^2/\text{g}$ , respectively, the Barret–Joyner-Halenda (BJH) adsorption surface area of the pores was  $165~\text{m}^2/\text{g}$  and the Langmuir surface area was  $2792~\text{m}^2/\text{g}$ . Other surface area models investigated include the Dollimore Heal Method (DH) cumulative adsorption surface area, Dubbin-Radushkevic Method (DR) micropore area, Density Functional Theory Method (DFT) and t-method external surface area with pore surface area values of  $175.1~\text{m}^2/\text{g}$ ,  $162~\text{m}^2/\text{g}$ ,  $33.97~\text{m}^2/\text{g}$  and  $159.4~\text{m}^2/\text{g}$ , respectively. This research is essential because a catalyst's surface area has a significant impact on the activity of the catalyst, since a catalyst's surface area affects how easily reactants interact with its active sites.

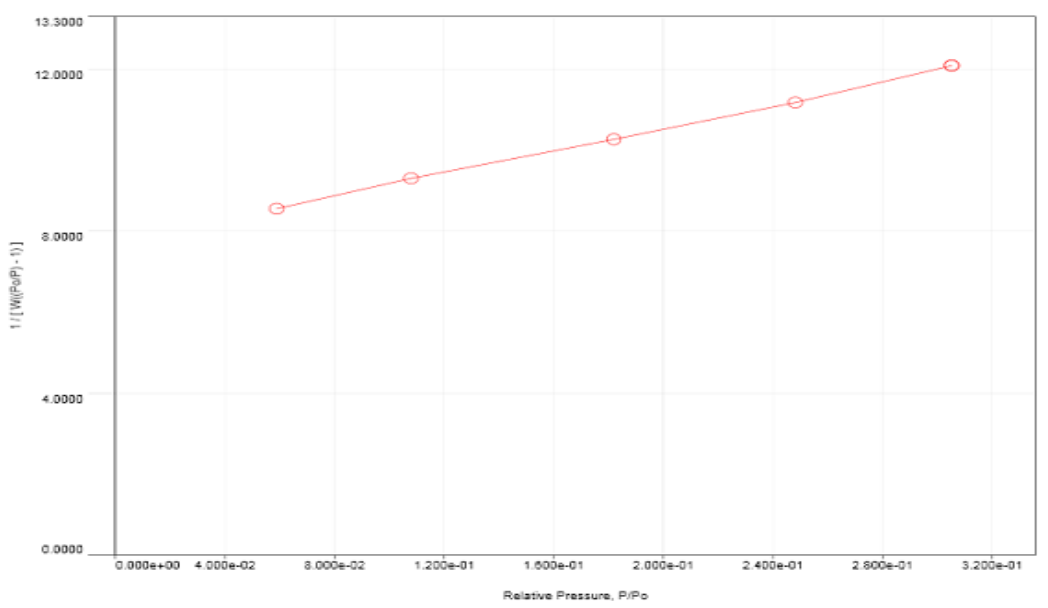


Figure 5. Multi Point BET plot for the bi-functional catalyst mean pore surface area.

#### 3.6.2. Pore volume

The mean pore volume analyzed using the BJH method was 812.5 cc/g while that of the DH, DR, and DFT methods were 830.4 cc/g, 575.9 cc/g and 411 cc/g respectively. Other methods used for analysis of the pore volume of the bi-functional catalysts included the Horvath-Kawazoe Method (HK) and the Saito-Foley Method (SF) with mean pore volumes of 225.4 cc/g and 378.5 cc/g respectively. Figure 6 shows the BJH plot for the mean pore volume of the bi-functional catalyst.

# 3.6.3. Pore diameter

The mean pore diameter analyzed using the Dubinin-Astakhov Method (DA) was 3.0 nm. Other methods employed in the analysis of the pore diameter were the BJH method, DH method, DR method, HK method, SF method and the DFT pore diameter method respectively with mean pore diameter values of 2.138 nm, 2.138 nm, 6.516nm, 1.847 nm, 3.488 nm and 2.647 nm. The DA pore diameter of 3.0nm falls within the mesoporous range, hence, it supports the adsorption-desorption isotherm of  $N_2$ .[18]. Figure 7 shows the DA method plot for the mean pore size/diameter distribution.

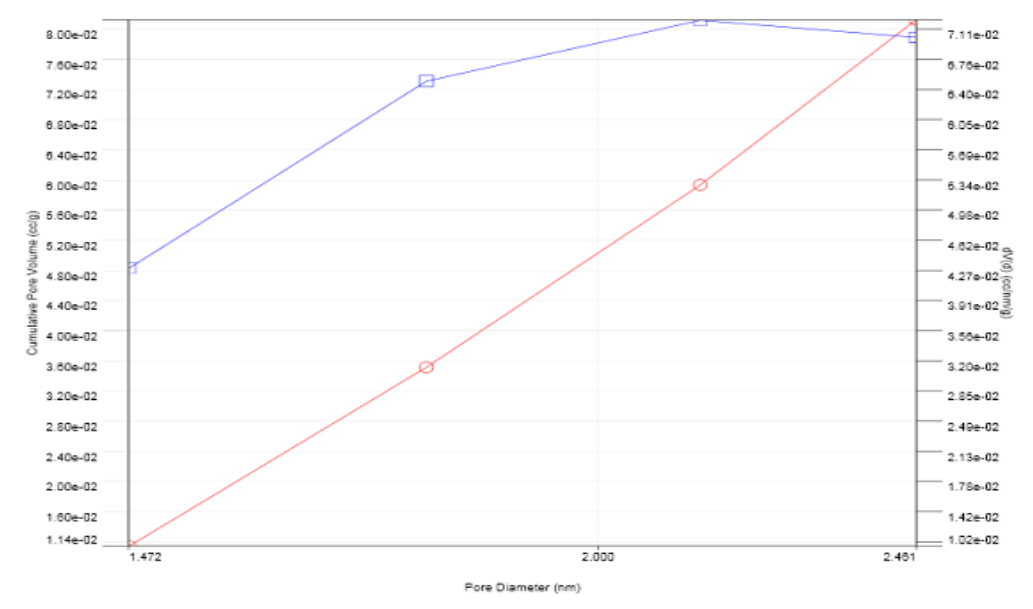


Figure 6. BJH method plot for Bi-functional catalyst mean pore volume.

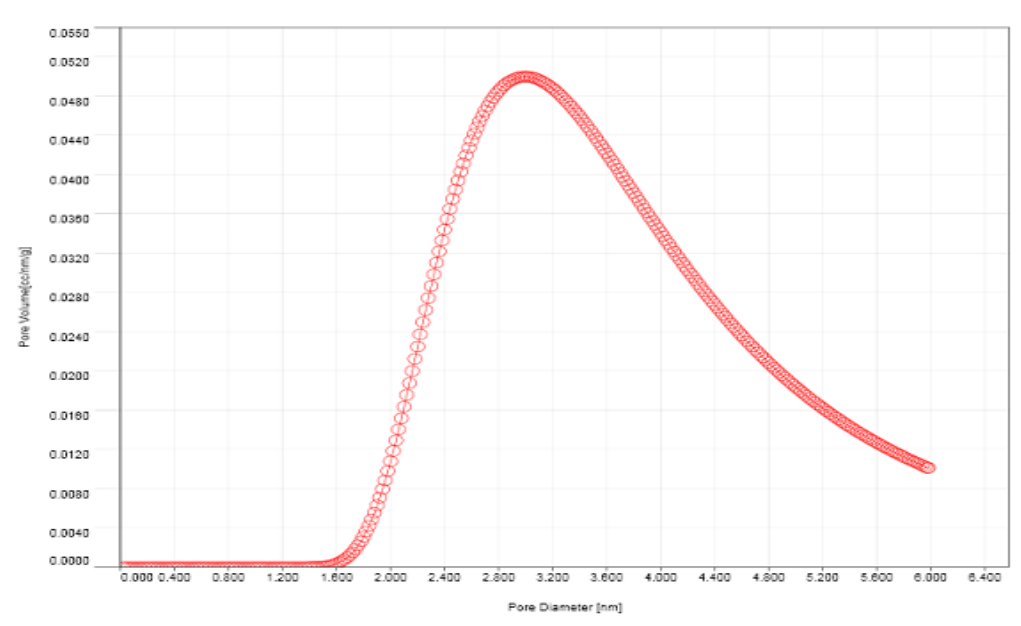


Figure 7. DA method plot for Bi-functional catalyst mean pore diameter.

# 4. CONCLUSION

This study successfully demonstrates the effective production of bi-functional catalysts leveraging agricultural waste materials as alkaline and acidic precursors. This research significantly advances the transformation of agricultural waste into valuable resources. By employing hydrothermal treatment on materials such as snail shells, eggshells, cocoa pods, and orange peels, the process generates both alkaline (CaO) and acidic precursors. These precursors serve as essential sites for bio-functional catalysts. This approach not only offers a sustainable method for managing waste but also opens doors for resource optimization. In summary, this study successfully demonstrates the creation of innovative bi-functional catalysts through a hydrothermal process. These catalysts exhibit favorable properties that make them ideal for a variety of applications, including organic synthesis, environmental cleanup, and biofuel generation.

# **ACKNOWLEDGEMENTS**

We would like to thank the Department of Chemical Engineering, University of Benin, Benin City, for providing us with research facilities.

# REFERENCES

- [1]. Zamani A.P., Marjani Z., and Mousavi Z.- Agricultural waste biomass-assisted nanostructures: Synthesis and application. Green Processing and Synthesis. **8** (1) (2019) 421-429. <a href="http://dx.doi.org/10.1515/gps-2019-0010">http://dx.doi.org/10.1515/gps-2019-0010</a>
- [2]. Andas J., Rahman M.L.A., and Yahya M.S.M. -Preparation and characterization of activated carbon from palm kernel shell. In IOP Conference Series: Materials Science and Engineering. **226** (1) (2017) 012156). <a href="http://dx.doi.org/10.1088/1757-899X/226/1/012156">http://dx.doi.org/10.1088/1757-899X/226/1/012156</a>
- [3]. Rashidi N.A., and Yusup S. -A review on recent technological advancement in the activated carbon production from oil palm wastes. Chemical Engineering Journal. **314** (2017) 277-290. https://doi.org/10.1016/j.cej.2016.11.059
- [4]. Mo J., Yang Q., Zhang N., Zhang W., Zheng Y and Zhang Z. -A review on agro-industrial waste (AIW) derived adsorbents for water and wastewater treatment. Journal of Environmental Management. 227 (2018) 395-405. http://doi.org/2010.1016/j.jenvman.2018.08.069
- [5]. Laca A., and Diaz M.- Eggshell waste as catalyst: A review. Journal of Environmental Management. 197 (2017) 351–359. <a href="https://doi.org/10.1016/j.jenvman.2017.03.088">https://doi.org/10.1016/j.jenvman.2017.03.088</a>
- [6]. Tan Y.H., Abdullah M.O., and Nolasco-Hipolito C. The potential of waste cooking oil-based biodiesel using heterogeneous catalyst derived from various calcined eggshells coupled with an emulsification technique: A review on the emission reduction and engine performance. Renewable and Sustainable Energy Reviews. 47 (2015) 589–603. <a href="https://doi.org/10.1016/j.rser.2015.03.048">https://doi.org/10.1016/j.rser.2015.03.048</a>
- [7]. Hamza M., Ayoub R.B., Shamsuddin A., Mukhtar S., Saqib I., Zahid M., and Ibrahim A.- review on the waste biomass derived catalysts for biodiesel production. Environmental Technology and Innovation. 21 (12) 2021 101200. https://doi.org/10.1016/j.eti.2020.101200
- [8]. Marwaha A., Rosha P., Mohapatra S.K., Mahla S.K., and Dhir A.- Waste materials as potential catalysts for biodiesel production: Current state and future scope. Fuel Process Technology. **181** (2018) 175–186. <a href="http://doi.org/10.1016/j.fuproc.2018.09.011">http://doi.org/10.1016/j.fuproc.2018.09.011</a>
- [9]. Mardhiah H. H., Ong H. C., Masjuki H. H., Lim S., and Lee H. V. A review on latest developments and future prospects of heterogeneous catalyst in biodiesel production from non-edible oils. Renewable Sustainable energy reviews. 67 (2017) 1225-1236. http://dx.doi.org/10.1016/j.rser.2016.09.036
- [10]. Jambhulkar D.K., Ugwekar R.P., Bhanvase B.A., and Barai D.P. A review on solid base heterogeneous catalysts: preparation, characterization and applications. Chemical Engineering Communication. **209** (6) (2020) 1-52. <a href="http://dx.doi.org/10.1080/00986445.2020.1864623">http://dx.doi.org/10.1080/00986445.2020.1864623</a>
- [11]. Hattori H.- Solid base catalysts: fundamentals and their applications in organic reactions. Appl. Catalalysis, General A. **504** (2015) 103–109. <a href="https://doi:10.1016/j.apcata.2014.10.060">https://doi:10.1016/j.apcata.2014.10.060</a>
- [12]. Din I.U., Nasir Q., Garba M.D.,, Alharthi A.A., Alotaibi M.A., and Usman M. A review of preparation methods for heterogeneous catalysts. Mini-Reviews in Organic Chemistry. **19** (1) (2022) 92-110. https://doi.org/10.2174/1570193X18666210308151136
- [13]. Li J., Wu Q., and Wu J.- Synthesis of Nanoparticles via Solvothermal and Hydrothermal Methods. Springer Nature. 12 (2015) 1-28. http://dx.doi.org/10.1007/978-3-319-15338-4 17

- [14]. Ulakpa W.C., Maryjane I. A., Augustine C.O., Olaseinde A.A., Odeworitse E., Onoriode E., Oluwatosin A.S., Olutoye A.M., Dim P., and Siddique M. Synthesis and characterization of calcium oxide nanoparticles (CaO NPS) from snail shells using hydrothermal method. Journal of the Turkish Chemical Society A. 11 (2) (2024) 825-34. https://doi.org/10.18596/jotcsa.1416214
- [15]. Enoch W., Mugisha P.J., Ratibu A., Wendiro D., Kyambadde J., and Vuzi P.C.- Spectroscopic Analysis of Heterogeneous Biocatalysts for biodiesel production from expired sunflower cooking oil .Journal of Spectroscopy. 4 (8) 2015. <a href="http://dx.doi.org/10.1155/2015/714396">http://dx.doi.org/10.1155/2015/714396</a>
- [16]. Simpen I.N., Winaya I.N.S., Subagia I.D.G.A., and Suyasa I.W.B.- Green nano-composite of CaO/K-Sulfated TiO<sub>2</sub> and Its potential as a single-step reaction solid catalyst for biofuel production. KnE Life Science. 7 (2022) 382-392. http://dx.doi.org/10.18502/kls.v7i3.11146
- [17]. Gaurav K., Kumari S., and Dutta J.- Utilization of waste chicken eggshell as heterogeneous CaO nanoparticle for biodiesel production. Journal of Biochemical Technology. **12** (1) (2021) 49–57. http://dx.doi.org/10.51847/eqTib7hM7Z
- [18]. Changmai B., Rano R., Vanlalveni C., and Rokhum L. A novel Citrus sinensis peel ash coated magnetic nanoparticles as an easily recoverable solid catalyst for biodiesel production. Fuel, **286** (2021) 119447. <a href="https://doi.org/10.1016/J.Fuel.2020.119447">https://doi.org/10.1016/J.Fuel.2020.119447</a>